ELSEVIER

Chemical Engineering Journal 122 (2006) 55–63

Chemical Engineering Journal

www.elsevier.com/locate/cej

Application of *Azolla rongpong* on biosorption of acid red 88, acid green 3, acid orange 7 and acid blue 15 from synthetic solutions

T.V.N. Padmesh [a], K. Vijayaraghavan [a], G. Sekaran [b], M. Velan [a,*]

[a] *Department of Chemical Engineering, Anna University, Chennai 600025, India*
[b] *Department of Environmental Technology, Central Leather Research Institute, Chennai 600020, India*

Received 14 July 2005; received in revised form 19 March 2006; accepted 28 March 2006

Abstract

Azolla rongpong, a fresh water macro alga, was tested for its ability to remove acid dyes (acid red 88 (AR88), acid green 3 (AG3), acid orange 7 (AO7) and acid blue 15 (AB15)) separately from aqueous solution. The sorption isotherms, obtained at different ranges of pH (2–3.5) and temperature (25–35 °C), were fitted using Langmuir, Freundlich, Redlich–Peterson and Sips models. The maximum dye uptake of 83.33 mg/g was obtained for AG3 at optimum conditions of pH (2.5) and temperature (30 °C) according to Langmuir isotherm model. Various thermodynamic parameters such as ΔG°, ΔH° and ΔS° were calculated indicating that the present system was spontaneous and endothermic process. The pseudo-first and -second order kinetic models were also applied to the experimental kinetic data obtained during biosorption of four acid dyes and high correlation coefficients favor pseudo-second order model for the present systems. Since *A. rongpong* performed very well in the case of AG3 biosorption compared to other dyes, AG3 was selected as the model dye for examining the potential of *A. rongpong* in continuous biosorption. A glass column (2 cm i.d. and 35 cm height) was used to conduct continuous experiments. At 25 cm (bed height), 5 mL/min (flow rate) and 100 mg/L (initial dye concentration), *A. rongpong* exhibited AG3 uptake of 84.87 mg/g. The experimental data were analyzed using Bed Depth Service Time and Thomas models and the model parameters were evaluated.

Keywords: Biosorption; Acid dyes; *Azolla rongpong*; Kinetics; Packed column

1. Introduction

Pollution caused by industrial wastewater has become a common problem for many countries. Especially, organic, inorganic and dye pollutions from industrial effluents disturb human health and ecological equilibrium [1]. Among various industries, the textile industry ranks first in the usage of dyes for coloration of the fibers. The textile sector alone consumes about 60% of total dye production for coloration of various fabrics and out of it, around 10–15% of the dyes used for coloration comes out through the effluents [2]. Based on chemical structure or chromophore, 20–30 different groups of dyes can be discerned. Acid dyes are anionic compounds that are mainly used for dyeing nitrogen-containing fabrics. The acid refers to the pH in acid dye baths rather then to the presence of acid groups (sulphonate, carboxyl) in the molecular structure [2].

The methods of color removal from industrial effluents include biological treatment, coagulation, flotation, adsorption, oxidation, hyper filtration, etc. [3]. Currently research community is focused on technologies for the treatment of polluted environments that are less costly and ecofriendly. All the conventional physical and chemical methods used for the biosorption are often cost prohibitive while biological methods are relatively cheap as well as ecofriendly [4].

Biosorption, the passive uptake of pollutants from aqueous solutions by the use of non-living microbial biomass, is a popular technique used for dye removal from wastewaters [4,5]. The main attractions of biosorption are high selectivity, cost effectiveness, high efficiency and good removal performance. Some important biosorbents used for dye removal include bacteria [6], fungi [7,8] and algae [9].

Algae have been widely used for the removal of heavy metal ions from solutions and they usually showed very high biosorption potential. However, the application of algae to dye removal was scarce. Macro fresh water algae, a renewable natural biomass, were commonly found in the many parts of the world. *Azolla*, one of the most commonly available fresh water algae, was the focus of the present study. This alga is commonly found in ditches, ponds and slow moving streams and is capable

* Corresponding author. Tel.: +91 44 222 03506; fax: +91 44 223 52642.
E-mail address: velan@annauniv.edu (M. Velan).

1385-8947/$ – see front matter © 2006 Elsevier B.V. All rights reserved.
doi:10.1016/j.cej.2006.05.013

of colonizing rapidly to form dense mats over water surfaces thus imposing negative effects on the aquatic ecology [10]. Thus, its usage in wastewater treatment is of interest and it may also add revenue to the local community. Furthermore, its macroscopic structure and rigid shape is particularly suitable for biosorption column applications.

The present study aims to investigate the biosorption potential of *Azolla rongpong* on the removal of acid dyes (acid red 88 (AR88), acid green 3 (AG3), acid orange 7 (AO7) and acid blue 15 (AB15)) from aqueous solutions in batch and continuous mode of operation.

2. Materials and methods

2.1. Biosorbent and chemicals

A. rongpong was collected from Agricultural University, Coimbatore, India. It was then sun dried and crushed to particle sizes in the range of 1–2 mm. The crushed particles were then treated with 0.1 M HCl for 5 h followed by washing with distilled water and then kept for shaded dry. The resultant biomass was subsequently used in sorption experiments. Acid red 88, acid green 3, acid blue 15 and acid orange 7 were obtained from Sigma–Aldrich Corporation, Bangalore, India. The properties of the dyes used are given in Table 1. The chemical structures of all four acid dyes are shown in Fig. 1.

Table 1
Properties of all four dyes used in this study

C.I. name	Molecular weight	λ_{max} (nm)	Molecular formula
Acid red 88	400.39	503	$C_{20}H_{13}N_2NaO_4S$
Acid green 3	690.82	636	$C_{37}H_{37}N_2O_6S_2Na$
Acid orange 7	350.33	452	$C_{16}H_{11}N_2NaO_4S$
Acid blue 15	775.96	564	$C_{42}H_{46}N_3NaO_6S_2$

2.2. Batch experiments

Batch biosorption experiments were performed in a rotary shaker at 150 rpm using 250 mL Erlenmeyer flasks containing 0.2 g of *A. rongpong* biomass in 50 mL of solution containing different dye concentration. After 12 h, the reaction mixture was centrifuged at 3000 rpm for 10 min. The dye content in the supernatant was determined using UV-Spectrophotometer (Hitachi,

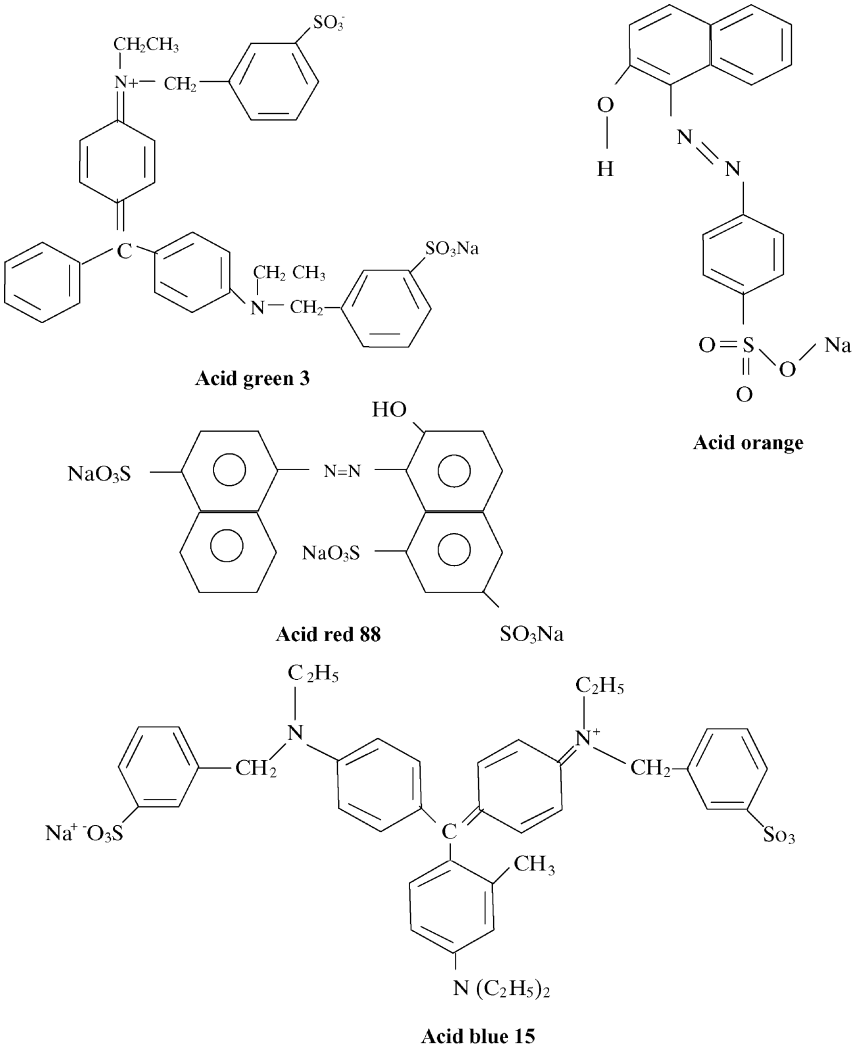

Fig. 1. The chemical structures of four acid dyes used in this study.

Japan) at λ_{max} 503, 564, 636 and 452 nm for AR88, AB15, AG3 and AO7, respectively. The amount of dye biosorbed was calculated from the difference between the dye quantity added to the biomass and the dye content of the supernatant using the following equation:

$$q_e = \frac{V}{M}(C_0 - C_f) \quad (1)$$

where q_e is the dye uptake (mg/g), C_0 and C_f the initial and final dye concentrations in the solution (mg/L), respectively, V the solution volume (L), and M is the mass of biosorbent (g).

2.3. Biosorption isotherm models

Four equilibrium isotherm models were used to fit the experimental data. These isotherms are the following:

$$\text{Langmuir model}: \quad q = \frac{q_{max} b C_f}{1 + bC_f} \quad (2)$$

$$\text{Freundlich model}: \quad q = K_F C_f^{1/n} \quad (3)$$

$$\text{Redlich–Peterson model}: \quad q = \frac{K_{RP} C_f}{1 + a_{RP} C_f^{\beta_{RP}}} \quad (4)$$

$$\text{Sips model}: \quad q = \frac{K_S C_f^{\beta_S}}{1 + a_S C_f^{\beta_S}} \quad (5)$$

where q_{max} is the maximum dye uptake (mg/g), b the Langmuir equilibrium constant (L/mg), K_F the Freundlich constant (L/g), n the Freundlich constant, K_{RP} the Redlich–Peterson isotherm constant (L/g), a_{RP} the Redlich–Peterson isotherm constant (L/mg), β_{RP} the Redlich–Peterson model exponent, K_S the Sips model isotherm constant (L/g), a_S the Sips model constant (L/mg) and β_S is the Sips model exponent. All the model parameters were evaluated by non-linear regression using MATLAB® software.

2.4. Batch kinetic models

The batch kinetic data were analyzed using pseudo-first [11] and pseudo-second order models [12]. The linearized form of pseudo-first and pseudo-second order model are shown below as Eqs. (6) and (7), respectively:

$$\log(q_e - q_t) = \log(q_e) - \frac{k_1}{2.303} t \quad (6)$$

$$\frac{t}{q_t} = \frac{1}{k_2 q_e^2} + \frac{1}{q_e} t \quad (7)$$

where q_e is the amount of dye sorbed at equilibrium (mg/g), q_t the amount of dye sorbed at time t (mg/g), k_1 the first-order rate constant (1/min), and k_2 is the second-order rate constant (g/mg min).

2.5. Column experiments

Fixed bed biosorption experiments were conducted in a glass column of internal diameter 2 cm and height 35 cm [13]. A known quantity of *A. rongpong* was packed in the column to yield the desired bed height of the sorbent. A peristaltic pump (Miclins) was used to pump the known concentration (100 mg/L) of dye solution (pH 2.5) through the column in the upward direction. The aliquot of dye at the outlet of the column was collected at regular time intervals. The operation of the column was stopped when the effluent dye concentration exceeded a value of 100 mg/L.

The breakthrough time (t_b, the time at which dye concentration in the effluent reached 1 mg/L) and bed exhaustion time (t_e, the time at which dye concentration in the effluent reached 100 mg/L) were used to evaluate the breakthrough curves. The slope of the breakthrough curve (dc/dt) was determined from t_b to t_e. The area above the break through curve (outlet dye concentration (C) versus time (t)) multiplied by the flow rate represents the quantity of dye retained in the column (m_{ad}). The uptake of the alga (q) can be determined by dividing the dye mass (m_{ad}) by the mass of the sorbent (M) [14,15]. The volume of the effluent (V_{eff}) can be calculated as follows:

$$V_{eff} = \frac{60}{1000} F t_e \quad (8)$$

where F is the volumetric flow rate (mL/min) and t_e is the exhaustion time (h).

Total amount dye sent to column (m_{total}) can be calculated as follows:

$$m_{total} = \frac{C_0 F t_e}{1000} \quad (9)$$

Total removal percent of dye with respect to flow volume can also be calculated as follows:

$$\text{Total dye removal (\%)} = \frac{m_{ad}}{m_{total}} \times 100 \quad (10)$$

All experimental data were the mean values of two replicate experiments.

3. Results and discussion

3.1. Batch studies

3.1.1. Biosorption isotherm

Fig. 2 represents the experimental dye biosorption isotherms for *A. rongpong* at different pH (2–3) and temperature (25–35 °C). The preliminary experiments were carried out in the pH range of 2–7 and for temperature 20–55 °C on all acid dyes using *A. rongpong* (data not shown). From the preliminary biosorption experiments, we observed that the maximum uptake of all acid dyes onto the *A. rongpong* was observed in the pH 2.5 and in the temperature 30 °C; hence biosorption isotherm experiments were conducted only in this pH and temperature ranges. For all acid dyes examined, uptake increased with pH up to 2.5 and then declined with further increase in pH. This may be due to nature of binding groups present in the alga and solution chemistry of the dye used [16]. In addition to pH, the dye biosorption uptake capacity of *A. rongpong* was also affected by temperature. Among the temperature conditions examined, room temperature (30 °C) favored biosorption. The dye biosorp-

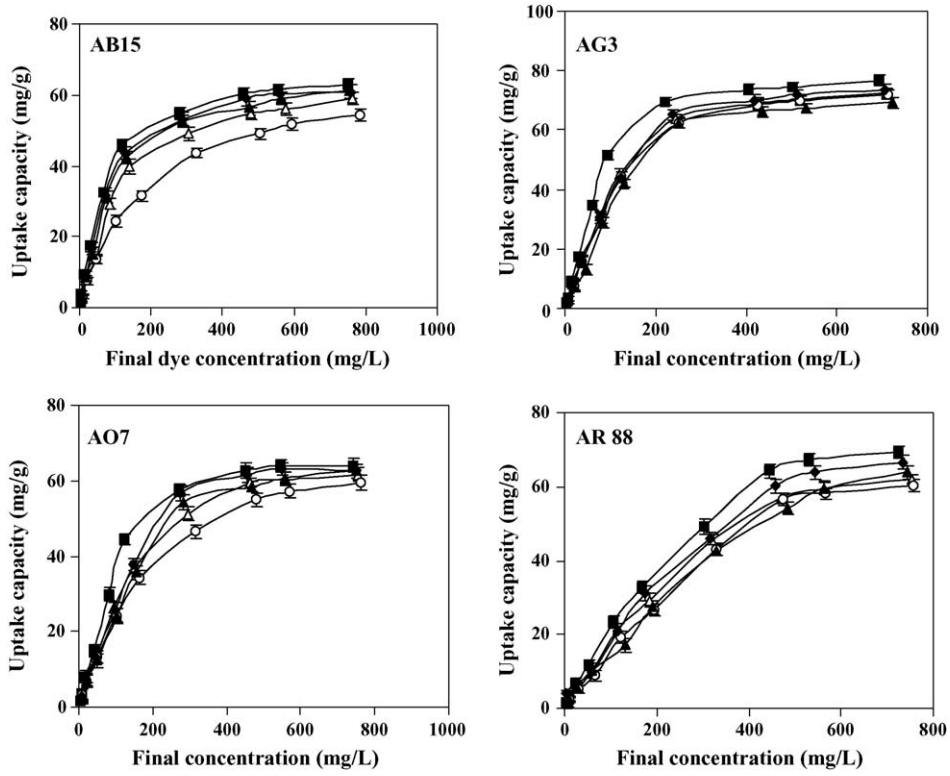

Fig. 2. Biosorption isotherms of AB15, AG3, AO7 and AR88 for *Azolla rongpong* at different conditions (biomass dosage = 4 g/L and agitation rate = 150 rpm). pH and temperature: (△) 2 and 30 °C; (■) 2.5 and 30 °C; (◯) 3 and 30 °C; (♦) 2.5 and 25 °C; (▲) 2.5 and 35 °C.

tion uptake capacity decreases by changing the temperature by ±5 °C from the room temperature.

Langmuir, Freundlich, Redlich–Peterson and Sips models were used to describe the non-linear equilibrium between the sorbed dye on the alga (q) and dye in the solution (C_f). The main reason for extended use of these isotherm models is that they incorporate constants that are easily interpretable. Table 2 shows the model constants along with correlation coefficients

Table 2
Langmuir, Freundlich, Redlich–Peterson and Sips model parameters at different conditions

Dye	Temperature (°C)	pH	Langmuir model			Freundlich model			Redlich–Peterson model				Sips model			
			Q_{max} (mg/g)	b (L/mg)	R^{2a}	K_F (L/g)	n	R^{2a}	K_{RP} (L/g)	a_{RP} (L/mg)	β_{RP}	R^{2a}	K_S (L/g)	a_S (L/mg)	β_S	R^{2a}
AB15	30	2.0	72.99	0.006	0.994	0.931	1.47	0.955	0.468	0.007	0.987	0.993	0.478	0.011	0.918	0.983
	30	2.5	76.34	0.011	0.999	1.790	1.68	0.945	0.870	0.017	0.943	0.992	0.880	0.013	0.993	0.986
	30	3.0	66.23	0.006	0.999	0.900	1.49	0.970	0.397	0.008	0.952	0.989	0.427	0.014	0.886	0.988
	25	2.5	62.11	0.011	0.998	1.360	1.58	0.963	1.240	0.226	0.473	0.987	1.390	0.304	0.444	0.975
	35	2.5	71.43	0.009	0.995	1.310	1.58	0.952	0.950	0.191	0.455	0.963	1.470	0.475	0.395	0.965
AG3	30	2.0	81.97	0.007	0.999	0.998	1.40	0.963	0.532	0.008	0.923	0.973	0.525	0.007	0.966	0.980
	30	2.5	83.33	0.009	0.999	0.712	1.47	0.944	1.450	0.018	0.989	0.985	1.170	0.019	0.946	0.984
	30	3.0	75.76	0.007	0.998	0.934	1.38	0.964	0.526	0.007	0.944	0.980	0.756	0.011	0.965	0.981
	25	2.5	79.37	0.007	0.997	1.060	1.01	0.969	0.530	0.004	0.980	0.989	0.539	0.005	0.990	0.984
	35	2.5	75.76	0.006	0.998	1.270	1.30	0.987	0.478	0.016	0.800	0.978	0.612	0.010	0.950	0.979
AR88	30	2.0	68.97	0.003	0.998	0.330	1.20	0.980	0.239	0.016	0.726	0.985	0.479	0.646	0.248	0.985
	30	2.5	81.30	0.004	0.999	0.483	1.26	0.981	0.316	0.018	0.757	0.986	0.673	0.512	0.322	0.979
	30	3.0	78.74	0.003	0.996	0.304	1.20	0.983	0.209	0.011	0.724	0.969	0.487	0.648	0.260	0.987
	25	2.5	71.43	0.004	0.999	0.270	1.24	0.952	0.730	0.410	0.570	0.989	1.400	0.325	0.571	0.977
	35	2.5	78.74	0.003	0.998	0.373	1.25	0.985	0.259	0.045	0.547	0.982	0.251	0.015	0.712	0.988
AO7	30	2.0	69.93	0.006	0.997	0.848	1.43	0.976	0.447	0.007	0.956	0.994	0.409	0.005	0.999	0.950
	30	2.5	76.92	0.007	0.998	1.070	1.47	0.957	0.578	0.011	0.930	0.996	0.538	0.007	0.978	0.984
	30	3.0	72.46	0.005	0.997	0.720	1.41	0.979	0.421	0.008	0.956	0.968	0.344	0.005	0.968	0.959
	25	2.5	72.99	0.005	0.999	0.680	1.29	0.972	0.551	0.261	0.306	0.996	0.941	0.890	0.229	0.989
	35	2.5	72.90	0.005	0.999	0.627	1.34	0.978	0.563	0.347	0.280	0.991	0.855	0.920	0.214	0.987

[a] Correlation coefficient.

obtain from four isotherm models. Langmuir sorption model served to estimate the maximum uptake values where they could not be reached in the experiments. Among four acid dyes, *A. rongpong* exhibited maximum uptake capacity for AG3. A maximum AG3 uptake of 83.33 mg/g was obtained at optimum pH (2.5) and temperature (30 °C) according to Langmuir model. The model fits the equilibrium data well at all conditions examined. To a minor extent, the Freundlich model also described the equilibrium data. Both Freundlich constants (K and $1/n$) also reached their maximum values at pH 2.5 and temperature = 30 °C. In the case of Redlich–Peterson model, correlation coefficients in the range of 0.968–0.996 were obtained and the model parameters varied with the conditions examined. Sips model described the equilibrium data reasonably well at all conditions examined. The Sips model constant, K_S, observed maximum at the optimum condition (2.5 and 30 °C), whereas other two constants (a_S and β_S) were lowest at this condition. The experimental results were analyzed statically using the Student's *t*-test [17]. From the test it was observed that for a 95% confidence level, the *t*-test value was equal to 2.672 (graph not shown). A typical example of batch biosorption isotherm fitted using four examined models is shown in Fig. 3.

3.1.2. Thermodynamic properties

Based on the fundamental thermodynamic properties, it is assumed that in an isolated system, energy cannot be gained or lost and the entropy change is the only driving force. In chemical engineering aspects, both energy and entropy factors must be considered in order to determine which process will occur spontaneously [18]. The Gibbs free energy change, ΔG°, is the fundamental criterion of spontaneity. It can be determined from:

$$\Delta G^\circ = -RT \ln b \quad (11)$$

where R is the gas constant (8.314 J/mol K) and T is the absolute temperature (K). The relationship between Gibbs free energy change, entropy change (ΔS°) and enthalpy change (ΔH°) can be expressed as:

$$\Delta G^\circ = \Delta H^\circ - T\Delta S^\circ \quad (12)$$

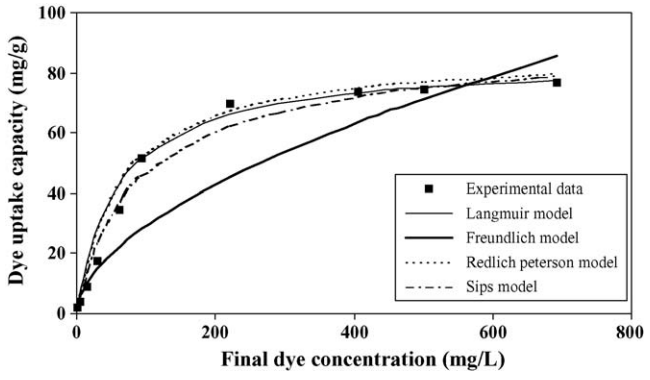

Fig. 3. Application of Langmuir, Freundlich, Redlich–Peterson and Sips models to experimental isotherm data obtained during AG3 biosorption by *A. rongpong* (pH 2.5, temperature = 30 °C, agitation rate = 150 rpm, biosorbent dosage = 4 g/L).

Table 3
Thermodynamic properties for all dyes

Dye	Temperature (°C)	ΔG (kJ/mol)	ΔS (kJ/mol K)	ΔH (kJ/mol)
AB15	25	−21.93	0.125	15.23
	30	−22.80		
	35	−23.18		
AG3	25	−20.64	0.173	30.98
	30	−21.37		
	35	−22.37		
AR88	25	−17.57	0.133	21.83
	30	−18.59		
	35	−18.89		
AO7	25	−18.50	0.148	25.82
	30	−18.81		
	35	−19.99		

The values of ΔG°, ΔH° and ΔS° are summarized in Table 3. For all acid dyes, the magnitude of ΔG° increases with increase in temperature. The negative value of ΔG° confirmed the feasibility of the process and the spontaneous nature of dye biosorption onto *A. rongpong*. The value of ΔH° was positive, indicating that the dye binding to alga was endothermic. This enthalpy change agrees well with those reported in the literature [18,19]. Also, the ΔS° was observed positive, indicating the increasing randomness at the solid/liquid interface during the biosorption [18].

3.1.3. Kinetic studies

Fig. 4 shows the kinetic data obtained during biosorption of acid dyes on *A. rongpong* at various initial concentrations. On exposing *A. rongpong* to dye solutions, it was observed that most of the process involving dye sorption was completed within 5–7 h followed by a slow process, which leads to the equilibrium dye concentration. While increasing the initial dye concentration, the total dye uptake increased whereas total percent removal decreased.

Pseudo-first and pseudo-second order models were used to describe kinetic biosorption data. The values of the predicted dye uptake capacity, rate constants along with correlation coefficients are presented in Table 4. For all acid dyes examined, correlation coefficients were found to be above 0.911, but the calculated Q_e is not equal to experimental Q_e, suggesting the insufficiency of pseudo-first order model to fit the kinetic data for the initial concentrations examined. The reason for these differences in the Q_e values is that there is a time lag, possibly due to a boundary layer or external resistance controlling at the beginning of the sorption process [20]. In most cases in the literature, the pseudo-first order model does not fit the kinetic data well for the whole range of contact time [20,21] and generally overestimate the Q_e values. The pseudo-second order model is based on the sorption capacity on the solid phase. Contrary to other well-established models, it predicts the behavior over the whole range of studies and it is in agreement with a chemisorption mechanism being the rate-controlling step. This was consistent with the better results obtained with the pseudo-second order model. On the basis of correlation coefficients values, it can

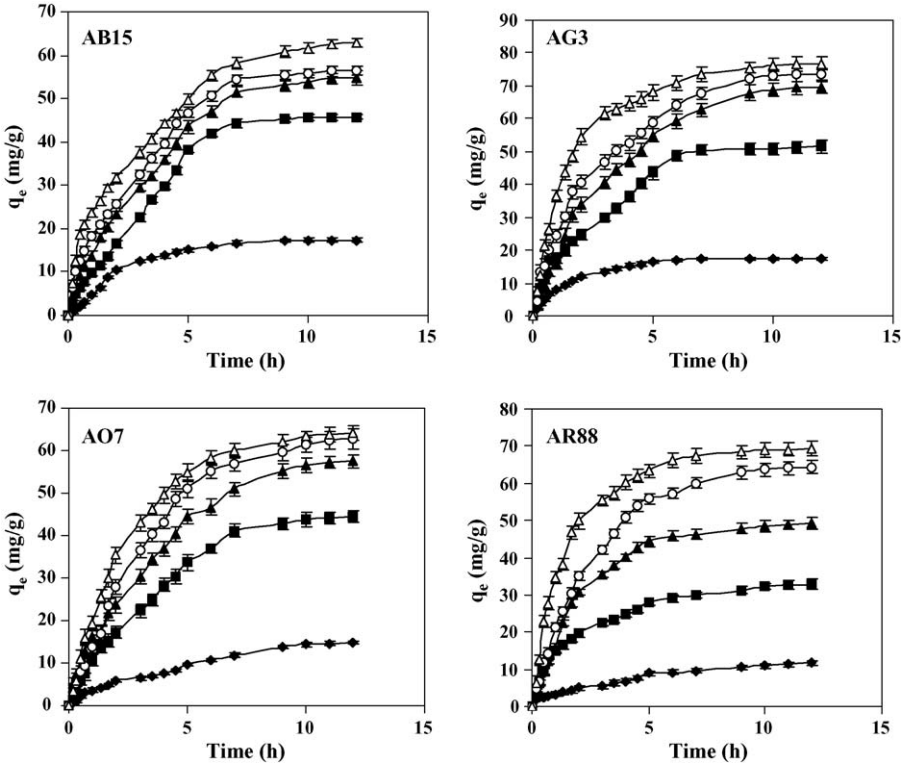

Fig. 4. Effect of initial AB15, AG3, AO7 and AR88 dye concentrations on the biosorption potential of *A. rongpong*. (♦) 100 mg/L; (■) 300 mg/L; (▲) 500 mg/L; (◯) 700 mg/L; (△) 1000 mg/L.

be concluded that pseudo-second order model may be suitable for the present systems. A typical example of batch biosorption kinetic data of AG3 fitted using two examined models is shown in Fig. 5.

3.2. Column studies

In the present study the biosorption efficiency sequence of *A. rongpong* increases in the following series: AR88 < AO7

Table 4
Kinetic parameters for the dye biosorption onto *Azolla rongpong* at different initial dye concentrations

Dye	Initial concentration (mg/L)	$(q_e)_{exp}$ (mg/g)	Pseudo-first order			Pseudo-second order		
			k_1 (L/min)	q_e (mg/g)	R^{2a}	k_2 (g/mg min)	q_e (mg/g)	R^{2a}
AB15	100	17.38	0.57	24.37	0.961	0.027	20.37	0.998
	300	45.77	0.59	50.98	0.928	0.013	52.08	0.995
	500	54.83	0.44	72.98	0.939	0.003	77.52	0.995
	700	60.17	0.47	76.49	0.961	0.002	81.30	0.997
	1000	62.83	0.41	83.56	0.959	0.002	87.72	0.997
AG3	100	17.42	0.61	18.61	0.986	0.040	19.76	0.998
	300	51.48	0.51	65.22	0.957	0.005	65.79	0.996
	500	69.62	0.44	91.41	0.948	0.003	94.34	0.996
	700	73.66	0.46	92.45	0.951	0.004	96.15	0.997
	1000	76.75	0.50	94.78	0.971	0.007	98.04	0.999
AR88	100	11.69	0.27	11.65	0.973	0.020	15.48	0.997
	300	32.80	0.40	32.28	0.948	0.020	37.04	0.997
	500	49.19	0.43	48.71	0.988	0.008	59.52	0.993
	700	64.25	0.49	78.87	0.963	0.004	82.64	0.993
	1000	69.22	0.52	81.28	0.991	0.007	87.72	0.992
AO7	100	14.80	0.33	18.64	0.911	0.082	21.98	0.998
	300	44.41	0.43	61.32	0.941	0.003	64.10	0.999
	500	57.45	0.43	76.21	0.920	0.002	83.33	0.993
	700	62.75	0.41	77.55	0.965	0.003	86.96	0.998
	1000	64.12	0.45	78.56	0.967	0.002	88.50	0.999

[a] Correlation coefficient.

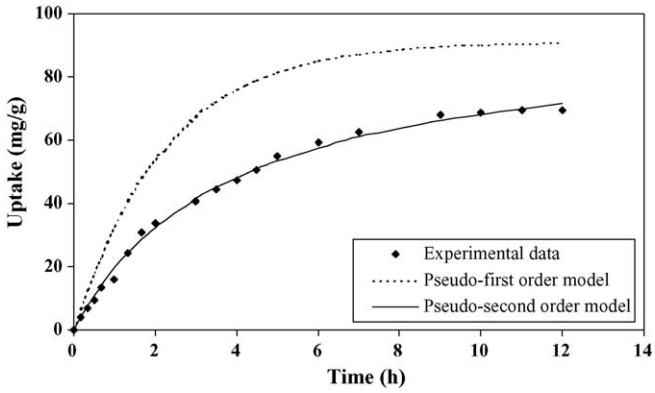

Fig. 5. Application of pseudo-first and pseudo-second order models to experimental kinetic data obtained during AG3 biosorption by *A. rongpong*. Conditions: pH 2.5, temperature = 30 °C, dye concentration = 500 mg/L, agitation rate = 150 rpm, biosorbent dosage = 4 g/L.

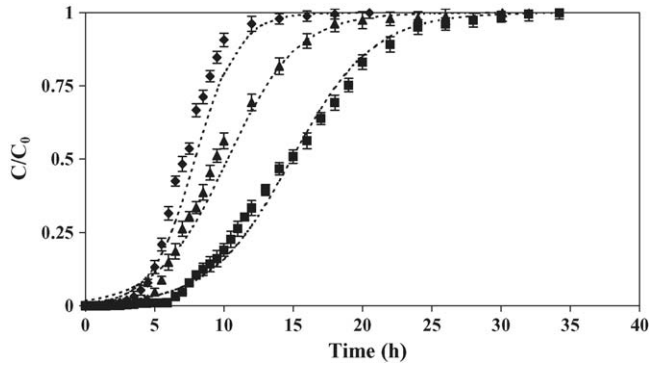

Fig. 6. Breakthrough curves for AG3 biosorption onto *A. rongpong* biomass at different bed heights (flow rate = 5 mL/min, initial AG3 concentration = 100 mg/L, pH 2.5). Bed heights: (♦) 15 cm; (▲) 20 cm; (■) 25 cm. (- - -) Predicted from Thomas model.

< AB15 < AG3. Therefore for examining the performance of *A. rongpong* on continuous removal, AG3 was selected as the model dye.

3.2.1. Effect of bed height

Biosorption of dyes in the packed bed column is largely dependent on the quantity of sorbent inside the column. Fig. 6 shows the break through curves for biosorption of AG3 by *A. rongpong* biomass at different bed heights. In order to yield different bed heights, 4.52, 6.14 and 7.89 g of biomass were added to produce 15, 20 and 25 cm, respectively. The inlet dye concentration (100 mg/L) and the flow rate (5 mL/min) were kept constant. Both breakthrough and exhaustion time increases as the bed height increases (Table 5) due to increase in the surface area of biosorbent. The AG3 uptake capacity of the biomass increases with the increase in the bed height as 56.56, 63.87 and 84.87 mg/g were observed at 15, 20 and 25 cm, respectively. Even though the breakthrough curves become steeper as the bed height decreased, a higher removal percentage was observed at the highest bed height.

The analysis of breakthrough curves was done using BDST model. The BDST is a simple model for predicting the relationship between bed height, Z, and service time, t, in terms of process concentrations and adsorption parameters [22]. The BDST approach is based on the Bohart–Adams equation. It is well established for dye adsorption in fixed bed systems [23,24]. Hutchins [25] proposed a linear relationship between bed height and service time given by Eq. (13):

$$t = \frac{N_0 Z}{C_0 v} - \frac{1}{K_a C_0} \ln\left(\frac{C_0}{C_b} - 1\right) \quad (13)$$

where C_b is the breakthrough dye concentration (mg/L), N_0 the sorption capacity of bed (mg/L), v the linear velocity (cm/h) and K_a is the rate constant (L/mg h). The column service time was chosen as the time when the effluent dye concentration reached 1 mg/L. The plot of service time against bed height at a flow rate of 5 mL/min (graph not presented) was linear ($R^2 = 0.992$), indicating the suitability of BDST model for the present system. The sorption capacity of the bed per unit bed volume (N_0), which was calculated from the slope of Eq. (13), was observed as 3821 mg/L. The rate constant, K_a, calculated from the intercept of BDST plot, was observed as 0.0111 L/mg h and it characterize the rate of solute transfer from the fluid phase to the solid phase [26].

3.2.2. Effect of flow rate

Flow rate is one of the important characteristics in evaluating sorbents for continuous-treatment of dyestuff effluents on an industrial scale [27]. The influence of flow rate on the biosorption of AG3 by *A. rongpong* was investigated by varying the flow rate from 5 to 15 mL/min (Fig. 7). The column performed well at the lowest flow rate and inferior column performance was observed as the flow rate increases (Table 5). This behavior may be due to insufficient time for the solute inside the column and the diffusion limitations of the solute into the pores of the sorbent at higher flow rates [28,29].

Table 5
Column data and parameters obtained at different bed heights, flow rates and initial dye concentrations

Dye	Bed height (cm)	Flow rate (mL/min)	Inlet dye concentration (mg/L)	t_b (h)	t_e (h)	Uptake (mg/g)	dc/dt (mg/L h)	V_{eff} (L)	Dye removal (%)
	15	5	100	1.9	20.5	56.56	6.883	6.15	41.57
	20	5	100	3.8	30.1	63.87	4.403	9.03	43.43
	25	5	100	5.9	34.2	84.87	4.143	10.26	65.27
AG3	25	10	100	3.5	23.8	82.30	5.477	7.14	45.47
	25	15	100	2.4	18.9	77.16	6.668	5.67	35.79
	25	5	50	8.2	63.8	48.95	1.098	19.74	40.36
	25	5	75	6.1	50.3	61.22	2.055	15.09	42.68

t_b: breakthrough time, t_e: bed exhaustion time and dc/dt: slope of the breakthrough curve.

Table 6
Thomas model parameters at different conditions

Dye	Bed height (cm)	Flow rate (mL/min)	Inlet dye concentration (mg/L)	Q_{exp} (mg/g)	Q_0 (mg/g)	k_{Th} (L/mg h)	R^{2a}
	15	5	100	56.56	56.55	0.006	0.992
	20	5	100	63.87	61.75	0.003	0.998
	25	5	100	84.87	81.99	0.002	0.993
AG3	25	10	100	82.30	81.88	0.005	0.996
	25	15	100	77.16	76.85	0.006	0.989
	25	5	50	48.95	48.41	0.004	0.999
	25	5	75	61.22	58.07	0.004	0.994

[a] Correlation coefficient.

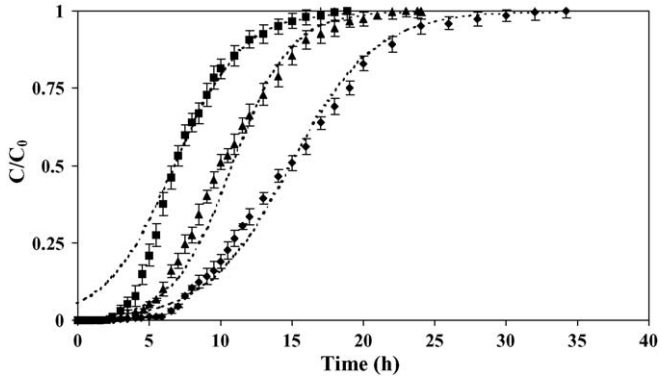

Fig. 7. Breakthrough curves for AG3 biosorption onto *A. rongpong* biomass at different flow rates (bed height = 25 cm, initial AG3 concentration = 100 mg/L, pH 2.5). Flow rates: (♦) 5 mL/min; (▲) 10 mL/min; (■) 15 mL/min. (- - -) Predicted from Thomas model.

3.2.3. Effect of initial dye concentration

The biosorption performance of *A. rongpong* was also examined at different inlet dye concentration. The breakthrough curves obtained by changing dye concentration from 50 to 100 mg/L at 5 mL/min flow rate and 25 cm bed height are shown in Fig. 8. A decreased inlet dye concentrations gave delayed breakthrough curves and the treated volume was also higher, since the lower concentration gradient caused the availability of reaction sites around or inside the biosorbent and also the slower transport due to decreased diffusion coefficient [15]. At the highest AG3 concentration (100 mg/L) the *Azolla* bed saturated quickly leading to earlier breakthrough and exhaustion time (Table 5). However, highest dye uptake value and steep breakthrough curves were obtained for 100 mg dye/L. The driving force for biosorption is the concentration difference between the dye on the biosorbent and the dye in the solution [15]. Thus the high driving force due to the high AG3 concentration resulted in better column performance.

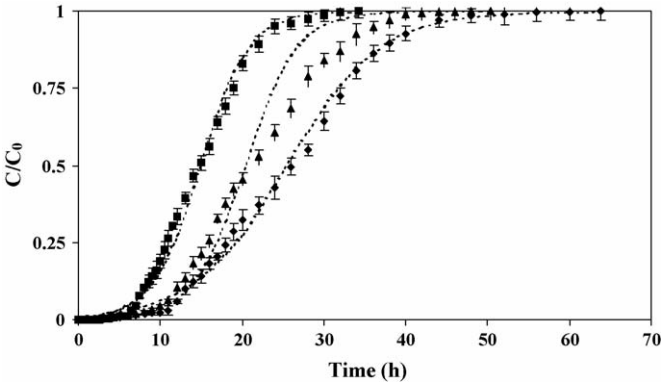

Fig. 8. Breakthrough curves for AG3 biosorption onto *A. rongpong* biomass at different concentrations (bed height = 25 cm, flow rate = 5 mL/min, pH 2.5). Initial dye concentrations: (♦) 50 mg/L; (▲) 75 mg/L; (■) 100 mg/L. (- - -) Predicted from Thomas model.

3.2.4. Application of the Thomas model

The prediction of breakthrough curve (C/C_0 versus t) is required for the successful design of a column sorption process [30]. The maximum adsorption capacity of an adsorbent is also needed in design. Various mathematical models can be used to describe fixed bed adsorption. Among these, the Thomas model, which was derived from the Bohart–Adams equation, is simple and widely used by several investigators and the model gives non-zero concentration at time, $t = 0$ [15,30,31].

The linearized form of Thomas model is expressed as follows:

$$\ln\left(\frac{C_0}{C} - 1\right) = \frac{k_{Th} Q_0 M}{F} - \frac{k_{Th} C_0}{F} V \quad (14)$$

where k_{Th} is the Thomas model constant (L/mg h), Q_0 the maximum solid-phase concentration of solute (mg/g) and V is the throughput volume (L). The model constants k_{Th} and Q_0 can be determined from a plot of $\ln[(C_0/C) - 1]$ against t at a given flow rate [15].

Comparison of experimentally determined and Thomas model predicted breakthrough curves are shown in Figs. 6–8. Table 6 summarizes the Thomas model parameters obtained at different bed heights, flow rates and initial AG3 concentrations. In general, good fits were obtained in all the cases with correlation coefficients ranging from 0.989 to 0.999. As bed height increases, the values of Q_0 increased and the values of k_{Th} decreased. The bed capacity Q_0 decreased and Thomas constant k_{Th} increased with increasing flow rate. In contrast, Q_0 increased and k_{Th} decrease with increasing initial AG3 concentration. In most cases a negligible difference between the experimental and predicted values of the bed capacity was observed.

4. Conclusion

A. rongpong was found to an efficient biosorbent for the removal of acid dyes from aqueous solutions. The solution pH and temperature strongly influenced the dye biosorptive capacity of *A. rongpong*. Among four isotherm models used, the Lang-

muir model better described the sorption isotherm. The kinetics of sorption at different initial dye concentrations is pseudo-second order with the parameters themselves directly varying with dye concentration. The column biosorption study using AG3 as model dye revealed bed height, flow rate and initial dye concentration affected biosorption behavior of *A. rongpong*. The BDST and Thomas models fitted the column biosorption data well. With easy availability and low cost as advantages, *A. rongpong* can become a suitable alternative for the treatment of acid dye-bearing wastewaters.

Acknowledgement

The authors are grateful to the Department of microbiology, Tamilnadu Agricultural University, Coimbatore, India, for providing the *A. rongpong* sample to the present study.

References

[1] A. Bilal, Batch kinetic study of sorption of methylene blue by pertile, Chem. Eng. J. 102 (2005) 73–81.
[2] H. Zollinger, Color Chemistry: Synthesis, Properties and Application of Organic Dyes and Pigments, VCH Publishers, New York, 2004.
[3] G. Mckay, J.F. Porter, G.R. Prasad, The removal of dye colors from aqueous solutions by adsorption on low cost materials, Wat. Air Soil Poll. 114 (1999) 423–438.
[4] S. Venkatamohan, N. Chandrasekhar Rao, Y.K. Krishna Prasad, J. Karthikeyan, Treatment of stimulated reactive yellow 22 (azo) dye effluents using *Spirogyra* species, Waste Manage. 22 (2002) 575–582.
[5] Z. Aksu, Application of biosorption for the removal of organic pollutants: a review, Proc. Biochem. 40 (3/4) (2004) 997–1026.
[6] T.L. Hu, Removal of reactive dyes from aqueous solution by different bacterial genera, Water Sci. Technol. 34 (1996) 89–95.
[7] K.A. Gallagher, M.G. Healy, S.J. Allen, Biosorption of synthetic dye and metal ions from aqueous effluents using fungal biomass, in: D.L. Wise (Ed.), Global Environmental Biotechnology, Elsevier, UK, 1997, pp. 27–50.
[8] Y. Fu, T. Viraraghavan, Removal of C.I. acid blue 29 from an aqueous solution by *Aspergillus niger*, AATCC Mag. 1 (2001) 36–40.
[9] Z. Aksu, S. Tezer, Biosorption of reactive dyes on the green alga *Chlorella vulgaris*, Proc. Biochem. 40 (2005) 1347–1361.
[10] T.V.N. Padmesh, K. Vijayaraghavan, G. Sekaran, M. Velan, Batch and column studies on biosorption of acid dyes on fresh water macro alga *Azolla filiculoides*, J. Hazard. Mater. B 125 (2005) 121–125.
[11] S. Lagergren, Zur theorie der sogenannten adsorption gelöster stoffe, K. Sevn. Vetenskapsakademiens. Handl. 24 (4) (1898) 1–39.
[12] G. Mckay, Y.S. Ho, Pseudo-second order model for sorption processes, Proc. Biochem. 34 (1999) 451–465.
[13] K. Vijayaraghavan, J. Jegan, K. Palanivelu, M. Velan, Removal of nickel(II) ions from aqueous solution using crab shell particles in a packed bed up-flow column, J. Hazard. Mater. 113B (2004) 223–230.
[14] B. Volesky, J. Weber, J.M. Park, Continuous-flow metal biosorption in a regenerable *Sargassum* column, Wat. Res. 37 (2003) 297–306.
[15] Z. Aksu, F. Gönen, Biosorption of phenol by immobilized activated sludge in a continuous packed bed: prediction of breakthrough curves, Proc. Biochem. 39 (2003) 599–613.
[16] P. Waranusantigul, P. Pokethitiyook, M. Kruatrachue, E.S. Upatham, Kinetics of basic dye (methylene blue) biosorption by giant duckweed (*Spirodela polyrrhiza*), Environ. Pollut. 125 (2003) 385–392.
[17] M.E.R. Carmona, M.A. Pereira da Silva, S.G.F. Leite, Biosorption of chromium using factorial experimental design, Proc. Biochem. 40 (2005) 779–788.
[18] Y.S. Ho, T.H. Chiang, Y.M. Hsueh, Removal of basic dye from aqueous solution using tree fern as a biosorbent, Proc. Biochem. 40 (2005) 119–124.
[19] N. Tewari, P. Vasudevan, B.K. Guha, Study on biosorption of Cr(VI) by *Mucor hiemalis*, Biochem. Eng. J. 23 (2005) 185–192.
[20] Y.S. Ho, G. McKay, Sorption of dye from aqueous solution by peat, Chem. Eng. J. 70 (1998) 115–124.
[21] Z. Reddad, C. Gerente, Y. Andres, P.L. Cloirec, Adsorption of several metal ions onto a low-cost biosorbent: kinetic and equilibrium studies, Environ. Sci. Technol. vol. 36 (2002) 2067–2073.
[22] Z. Zulfadhly, M.D. Mashitah, S. Bhatia, Heavy metals removal in fixed-bed column by the macro fungus *Pycnoporus sanguineus*, Environ. Pollut. 112 (2001) 463–470.
[23] G.M. Walker, L.R. Weatherley, Adsorption of acid dyes on to granular activated carbon in fixed beds, Wat. Res. 31 (1997) 2093–2101.
[24] G.M. Walker, L.R. Weatherley, COD removal from textile industry effluent: pilot plant studies, Chem. Eng. J. 84 (2001) 125–131.
[25] R.A. Hutchins, New method simplifies design of activated carbon systems, Chem. Eng. 80 (1973) 133–138.
[26] D.O. Cooney, Adsorption Design for Wastewater Treatment, CRC press, Boca Raton, 1999.
[27] M. Zhao, J.R. Duncan, R.P. Van Hille, Removal and recovery of zinc from solution and electroplating effluent using *Azolla filiculoides*, Wat. Res. 33 (1999) 1516–1522.
[28] D.C.K. Ko, J.F. Porter, G. McKay, Optimised correlations for the fixed-bed adsorption of metal ions on bone char, Chem. Eng. Sci. 55 (2000) 5819–5829.
[29] K. Vijayaraghavan, J. Jegan, K. Palanivelu, M. Velan, Biosorption of cobalt(II) and nickel(II) by seaweeds: batch and column studies, Sep. Purif. Technol. 44 (2005) 53–59.
[30] G. Yan, T. Viraraghavan, Heavy metal removal in a biosorption column by immobilized *M. rouxii* biomass, Biores. Technol. 78 (2001) 243–249.
[31] K. Vijayaraghavan, J. Jegan, K. Palanivelu, M. Velan, Batch and column removal of copper from aqueous solution using a brown marine alga *Turbinaria ornata*, Chem. Eng. J. 106 (2) (2005) 177–184.